Mice overexpressing BAFF develop a commensal flora–dependent, IgA-associated nephropathy

Douglas D. McCarthy,[1] Julie Kujawa,[2] Cheryl Wilson,[2] Adrian Papandile,[2] Urjana Poreci,[2] Elisa A. Porfilio,[1] Lesley Ward,[1] Melissa A.E. Lawson,[3] Andrew J. Macpherson,[3] Kathy D. McCoy,[3] York Pei,[4] Lea Novak,[5] Jeannette Y. Lee,[6] Bruce A. Julian,[5] Jan Novak,[5] Ann Ranger,[2] Jennifer L. Gommerman,[1] and Jeffrey L. Browning[2]

[1]Department of Immunology, University of Toronto, Toronto, Ontario, Canada. [2]Department of Immunobiology, Biogen Idec, Cambridge, Massachusetts, USA. [3]Farncombe Family Digestive Health Research Institute, McMaster University, Hamilton, Ontario, Canada. [4]Divisions of Nephrology and Genomic Medicine, University Health Network and University of Toronto, Ontario, Canada. [5]Departments of Pathology, Medicine, and Microbiology, University of Alabama at Birmingham, Birmingham, Alabama, USA. [6]Department of Biostatistics, University of Arkansas for Medical Sciences, Little Rock, Arkansas, USA.

B cell activation factor of the TNF family (BAFF) is a potent B cell survival factor. BAFF overexpressing transgenic mice (BAFF-Tg mice) exhibit features of autoimmune disease, including B cell hyperplasia and hypergammaglobulinemia, and develop fatal nephritis with age. However, basal serum IgA levels are also elevated, suggesting that the pathology in these mice may be more complex than initially appreciated. Consistent with this, we demonstrate here that BAFF-Tg mice have mesangial deposits of IgA along with high circulating levels of polymeric IgA that is aberrantly glycosylated. Renal disease in BAFF-Tg mice was associated with IgA, because serum IgA was highly elevated in nephritic mice and BAFF-Tg mice with genetic deletion of IgA exhibited less renal pathology. The presence of commensal flora was essential for the elevated serum IgA phenotype, and, unexpectedly, commensal bacteria–reactive IgA antibodies were found in the blood. These data illustrate how excess B cell survival signaling perturbs the normal balance with the microbiota, leading to a breach in the normal mucosal-peripheral compartmentalization. Such breaches may predispose the nonmucosal system to certain immune diseases. Indeed, we found that a subset of patients with IgA nephropathy had elevated serum levels of a proliferation inducing ligand (APRIL), a cytokine related to BAFF. These parallels between BAFF-Tg mice and human IgA nephropathy may provide a new framework to explore connections between mucosal environments and renal pathology.

Introduction

The generation of IgA in the mucosal compartments is a dominant immunological process that is crucial for homeostasis between the gut commensal flora and the local immunological environment (1, 2). This balance is certainly important for the proper functioning of the intestine, yet surprisingly, the composition of the gut microbiota can globally influence the immune system and disease development in nonmucosal organs (3). Mucosal IgA production occurs in the Peyer's patches (PPs), mesenteric lymph nodes (MLNs), and isolated lymphoid follicles (ILF), and these are the major inductive sites for IgA production (1, 4). Class switching to IgA can also occur in the gut lamina propria (LP) in mice and humans, although involvement of the latter setting is contentious. Stromal support cells within the LP have the capacity to induce class switching due to secretion of pro-IgA cytokines, inducing activation of LP B cells, and probably local expansion of plasma cells (PCs) (1, 5). Thus, the balance of various factors in the mucosal microenvironment plays an important role in regulating the synthesis of IgA.

Changes are observed in the IgA system in several pathological conditions. In IgA nephropathy (IgAN) and Henoch-Schönlein purpura nephritis, polymeric IgA-containing immune complexes are deposited in the kidney glomeruli, triggering renal injury (6). Serum IgA anti-gluten and anti-transglutaminase antibodies are observed in celiac disease, and serum IgA levels can be elevated in inflammatory bowel disease (7, 8). IgA pemphigus appears to be driven by direct autoreactivity, and the circulating level of IgA rheumatoid factor has a high prognostic value in rheumatoid arthritis (9, 10). In so-called seronegative lupus nephritis, a "full house" nephropathy pattern can be frequently observed that includes IgA deposition in the glomeruli (11). In the case of IgAN, the source of the IgA-producing PCs has been variously speculated to involve mucosal tissues, tonsils, and bone marrow. In IgAN, the IgA itself is not generally viewed as being autoreactive per se, but rather it has a strong propensity to form macromolecular complexes that accumulate as immuno-deposits in the glomerular mesangium (12). An analysis of O-linked glycosylation in the heavy chain hinge region of IgA1 revealed that serum and mesangial IgA1 is typically galactose deficient compared with that of normal serum IgA1, and some patients with IgAN have elevated circulating IgA (13–17). Despite considerable investigation into the biochemical abnormalities of IgA1 from patients with IgAN, the origin and localization of PCs secreting the aberrant IgA1, and the downstream effector mechanisms triggered by mesangial IgA1 deposition, the etiology of IgAN remains poorly understood.

Authorship note: Douglas D. McCarthy and Julie Kujawa contributed equally to this work. Ann Ranger, Jennifer L. Gommerman, and Jeffrey L. Browning are co–senior authors.

Conflict of interest: The authors have declared that no conflict of interest exists.

Citation for this article: *J Clin Invest.* 2011;121(10):3991–4002. doi:10.1172/JCI45563.

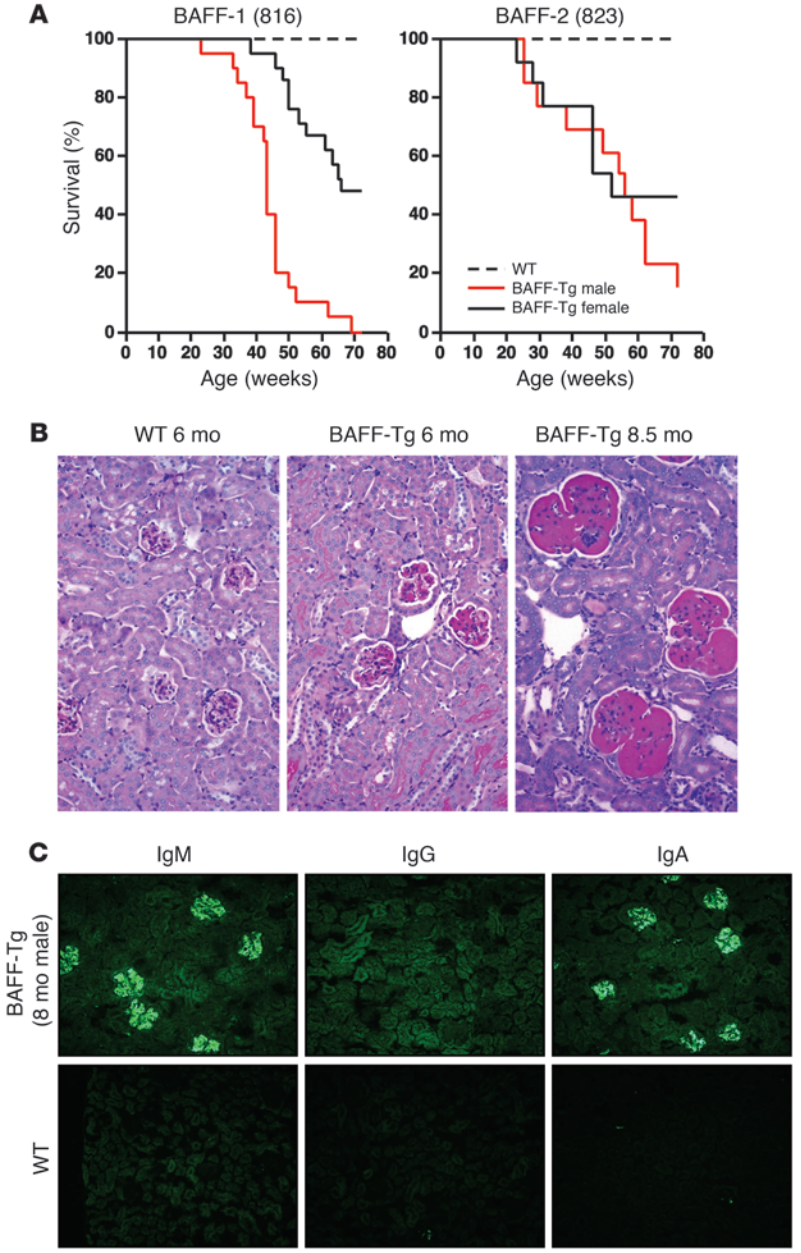

Figure 1
Gender-biased development of fatal nephropathy associated with dominant IgA and IgM glomerular deposits in the BAFF-Tg mice. (**A**) Cohorts of male and female BAFF-Tg mice and WT controls (n = 13–20 each) were observed for up to 21 months. Cohorts of BAFF-Tg mice for the survival experiments were derived from 2 homozygous founders called BAFF-1 (original 816 line) and BAFF-2 (original 823 line) (35), which had been rederived after receipt from the Garvan Institute. Genome scanning showed that both lines retained some DBA2 from the original transgenic derivation using DBA2 × B6 F_1 mice (BAFF-1, 10%; BAFF-2, 18%). The longitudinal study shown here was conducted from 2003 to 2005. This study was repeated from 2006 to 2008, and although onset of severe nephropathy was roughly equivalent (30–40 weeks) and the gender bias was present, we observed enhanced survival at the experiment end compared with that of the 2003 to 2005 cohort (data not shown). The improved survival was also recapitulated in BAFF-1 homozygous mice that retained only 4% DBA2 (see further discussion of this topic in the Methods). (**B**) Representative WT (6 months) and BAFF-2 Tg kidney tissues reveal increased mesangial matrix in BAFF-Tg mice (PAS stain; original magnification, ×200). (**C**) Representative IgA, IgG, and IgM deposits in BAFF-1 Tg mice versus WT mice (original magnification, ×200).

The controlling factors and microenvironmental signals that drive the massive switch to IgA in the gut have been extensively investigated. TGF-β is considered to be a requisite factor (18), and, more recently, signaling induced by the TNF family members B cell activation factor of the TNF family (BAFF; also known as BlyS) and APRIL has been implicated (1, 19–21). The B cell survival factor BAFF is produced by multiple cell types, including monocytes, dendritic cells, neutrophils, astrocytes, and stromal cells, and it interacts with 3 different receptors (BAFF receptor [BAFF-R], transmembrane activator and CAML interactor [TACI], and B cell maturation antigen [BCMA]) found predominantly on B cell lineages (22). In mice, survival function in transitional and mature B cell subsets is principally mediated by BAFF-R. With respect to IgA production, BAFF has been shown to induce T-independent class switching to both IgA and IgG (21), and BAFF can have a profound effect on IgA production (23–26). Moreover, recent work has shown that the APRIL-TACI axis is critical for IgA production in mice (19, 20) and humans (27, 28), and MyD88 can directly couple TACI to B cell class switch (29). These observations, combined with the dramatically enhanced IgA responses in vivo in BAFF overexpressing transgenic mice (BAFF-Tg mice) or recombinant BAFF-dosed mice (23, 24), have led to the hypothesis that APRIL, BAFF, or both play a substantial role in vivo in IgA class switching.

In the presence of excess BAFF, as in BAFF-Tg mice, some B cell subsets expand abnormally and B cell tolerance to self-antigen is perturbed (22). With age, the mice develop manifestations of autoimmune disease with features of SLE and Sjögren's syndrome. However, despite these compelling observations linking BAFF overexpression to autoimmunity, there were hints that the picture was more complex. While increases in serum levels of IgG and

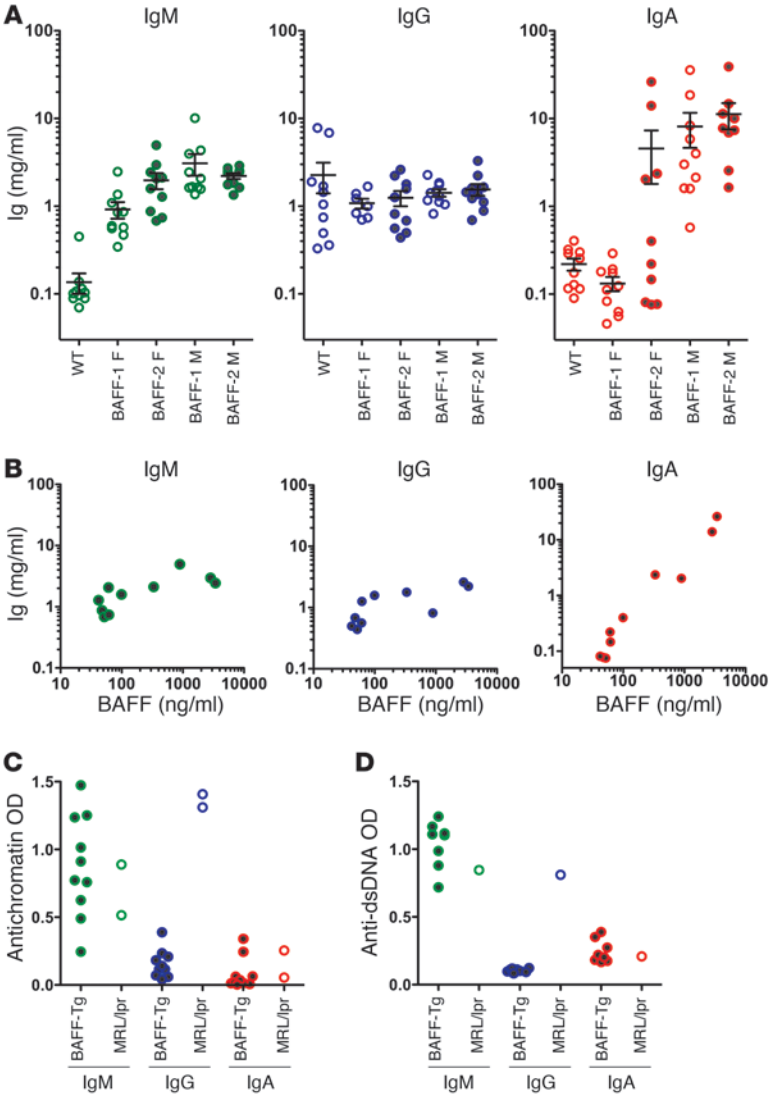

Figure 2
Dramatically elevated serum IgA in BAFF-Tg mice correlating with serum BAFF levels. Autoreactivity is limited to the IgM isotype. (**A**) Serum IgM, IgG, and IgA levels in a cohort of BAFF-1 Tg mice and BAFF-2 Tg mice at 3 to 4 months of age compared with those of matched WT controls. (**B**) Serum levels of IgA, but not IgM or IgG, are correlated with serum BAFF levels, as measured by ELISA in the BAFF-2 female cohort in **A**. (**C**) Antinuclear autoreactivity is observed only in the IgM isotype in BAFF-1 Tg mice. Antichromatin and (**D**) anti-dsDNA antibodies were evaluated in male BAFF-1 Tg mice and C57BL/6 mice (both 6 months old). Open circles show serum autoantibody levels from a diseased 3-month-old MRL/lpr mouse for reference. Individual symbols represent individual mice; horizontal bars represent the mean ± SEM. F, female; M, male.

antinuclear antibodies are modest, basal serum IgA levels are remarkably elevated in BAFF-Tg mice (25, 26). In light of these considerations, we reexamined the underlying pathology that was affecting survival in BAFF-Tg mice, with particular attention to the nature of the IgA. We considered the possibility that homeostatic immune responses to commensal flora may be an important variable in the manifestations of disease in BAFF-Tg mice. Indeed, inappropriate host responses to commensal organisms have been linked to autoimmune disorders, such as inflammatory bowel disease (30). Here, we show that BAFF-Tg mice develop an IgA-driven nephritis, and the development of this condition, which is commensal dependent, involves a breakdown in the normal barrier between the mucosal and peripheral compartments.

Results

BAFF-Tg mice develop glomerulonephritis with dominant IgA deposits. BAFF-Tg mice from 2 independently derived lines had a shortened lifespan in our colony, and most mice developed fatal/severe nephritis by 17 months of age (Figure 1A). Surprisingly, we observed a gender bias in disease progression, with males developing disease faster than females, especially in the BAFF-1 line. Upon examination, we found that serum BAFF levels were higher in male BAFF-Tg mice relative to those of their female counterparts (Supplemental Figure 1, A and B; supplemental material available online with this article; doi:10.1172/JCI45563DS1). To rule out a consumption effect, we evaluated the level of *BAFF* mRNA in spleen, liver, and kidney by quantitative real-time PCR (qPCR). While endogenous splenic *BAFF* mRNA levels were similar between males and females, transgenic expression of BAFF was markedly elevated in male liver and kidney relative to that of the female BAFF-Tg mice. The greatest differences were observed in the kidney (Supplemental Figure 1D). We suspect that the gender bias in BAFF expression is due to sexual dimorphism in the kidney expression of the α1-antitrypsin (*AAT*) gene cluster (see Supplemental Methods for more information). Thus, the correlation between lower BAFF levels and slower disease progression suggests that a critical amount of BAFF is necessary to drive the disease process.

By 6 months of age, most BAFF-Tg mice exhibited modest albuminuria (>30–100 mg/dl), with a mild renal histopathology that differed clearly from that observed in more conventional lupus mice such as (NZB × NZW)F_1 or MRL/lpr mice. The BAFF-Tg kidneys were characterized by segmental multifocal expansion of the mesangial matrix with hyaline material (PAS^+) (Figure 1B). Rare mild mesangial cell proliferation was observed; however, there was no glomerular sclerosis, tubular atrophy, or interstitial perivascular infiltration. With age, the mice developed more substantial albuminuria (>300 mg/dl) and displayed severe, global, and diffuse deposition of hyaline material in the glomeruli. At this stage, the kidneys were characterized by expanded glomeruli, occasional mesangial cell proliferation, and glomerular capillary thickening but no sclerosis. There was mild focal tubular atrophy that appeared to correlate with proteinuria, and dense perivascular lymphocytic infiltrates were present. Immunofluorescence analysis of kidney sections of BAFF-Tg mice with mild proteinuria at 6 to 8 months showed that all mice had substantial mesangial deposits of IgM in the glomeruli (Figure 1C and Supplemental Figure 2). By 8 months of age, coincident with an increase in proteinuria, most mice exhibited IgA mesangial deposition in the glomeruli, with varying degrees of IgG deposition, as described previously (26). Consistent with the paucity of

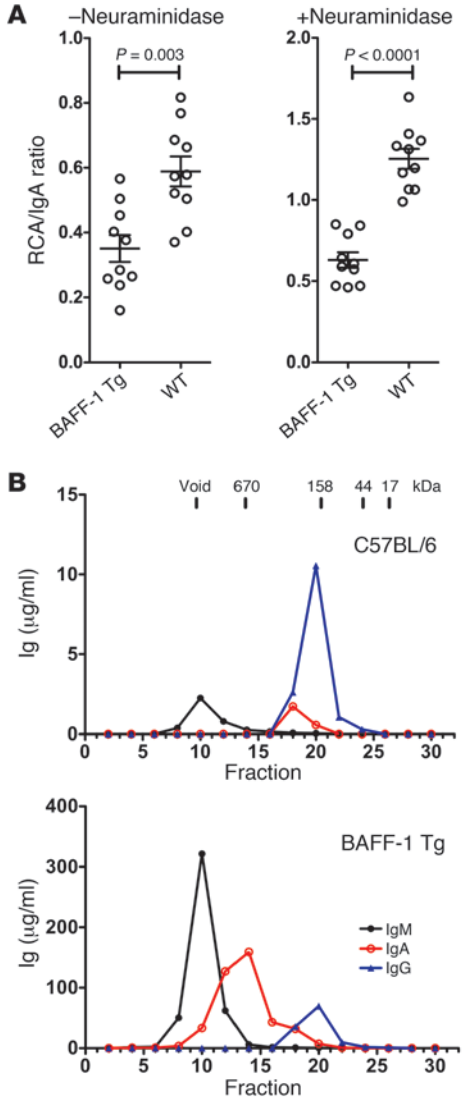

Figure 3
Accumulation of underglycosylated IgA and polymeric IgA in the serum of BAFF-Tg mice. (**A**) After IgA capture with an isotype-specific antibody, samples were or were not pretreated with neuraminidase, and the glycosylation state was then probed with RCA-1 lectin to detect terminal galactose residues. Relative levels of glycosylation are expressed as a binding ratio (OD lectin detection/OD anti-Ig detection). For reference, a mouse myeloma monoclonal IgA that had low levels of terminal galactose gave ratios of 0.1 and 0.25 (– and + neuraminidase, respectively). Individual symbols represent individual mice; horizontal bars represent the mean ± SEM. (**B**) Size-exclusion chromatography fractionation of IgA in sera of male C57BL/6 and male BAFF-1-Tg mice, showing the highly polymeric nature of the IgA and increased concentration of IgM in the BAFF-Tg mice.

IgG in the glomeruli, there was little C4 deposition. These results contrast with those for (NZB × NZW)F_1 mice, a traditional model of lupus, in which IgG and C4 deposits are readily observed in the kidney glomeruli (ref. 31 and Supplemental Figure 2). Age-matched control mice often showed modest glomerular deposits of IgM and some C4 with no apparent disease, as measured by the aforementioned histological parameters.

Absence of elevated serum IgG or antinuclear IgG antibodies in BAFF-Tg mice. Given the modest staining for IgG in the kidney glomeruli of the BAFF-Tg mice, we examined the serum Ig isotypes in these mice. Serological examination of mice at 3 months of age revealed that the most dramatic Ig elevations were in IgA and IgM (Figure 2A). Surprisingly, basal IgG levels were only slightly elevated or unchanged in these BAFF-Tg mice. The IgA and IgM levels generally became elevated relatively early (by 8 weeks) and remained at nearly the same level until 6 to 8 months, at which point, IgA levels begin to drop (Supplemental Figure 8A). In most BAFF-1 and some BAFF-2 Tg female mice, the IgA levels did not rise, and, indeed, serum IgA tracked with the serum BAFF levels (Figure 2B). While low serum levels of transgenic BAFF were sufficient to elevate IgM, IgA levels continued to increase with higher levels of BAFF. Because BAFF levels correlated directly with IgA levels and roughly with renal pathology, these findings suggested that IgA may contribute to the pathogenesis of nephropathy in BAFF-Tg mice.

Because BAFF-Tg mice had limited deposition of IgG or C4 in the kidney and relatively normal or modestly elevated levels of circulating IgG, we next examined whether these mice had elevated titers of antinuclear IgG antibodies, as has been previously reported (32, 33). In the current colonies (both at Biogen Idec and University of Toronto), substantial titers of IgG or IgA directed against antichromatin, dsDNA, ssDNA, and extractable nuclear antigen were not observed in either BAFF-Tg line (Figure 2, C and D, Supplemental Figure 3, and data not shown), especially when compared with autoimmune sera from the MRL/lpr mouse. Only IgM autoreactivity was observed in ELISA and crithidia formats, consistent with the observation that IgG autoreactivity may require collaboration between BAFF and other autoimmune loci (34). Therefore, in contrast to the original BAFF-Tg mice with more severe autoimmune manifestations (35), mice in the current colony did not exhibit hallmarks of classical autoreactive IgG-driven lupus nephritis but rather develop an IgA-associated kidney disease.

Characterization of serum IgA from BAFF-Tg mice. Because reduced glycosylation appears to be involved in the pathogenesis of human IgAN, the quality of the glycosylation of IgA in BAFF-Tg sera was probed using the galactose-recognizing lectin *Ricinus communis* agglutinin I (RCA) in an ELISA format (36). IgA from BAFF-Tg mice exhibited an approximately 50% reduction in RCA binding compared with that of WT control IgA, regardless of whether the sugars were desialylated with neuraminidase treatment (Figure 3A). Similar data were obtained using the sialic acid–specific lectin *Sambucus nigra* lectin, indicating less terminal sialic acid in IgA from BAFF-Tg mice (data not shown). These data indicate that serum IgA in BAFF-Tg mice is aberrantly glycosylated, with reduced amounts of terminal galactose and sialic acid.

Next, we evaluated the size of IgA and found that, compared with that of the WT control, serum from BAFF-Tg mice exhibited a substantial increase in polymeric IgA upon size fractionation, with the bulk of the IgA being at least 670 kDa, yet generally smaller than IgM (Figure 3B). SDS-PAGE analysis showed that the polymeric IgA did not dissociate in the presence of detergent, suggesting that its size was not due to immune complex formation (Supplemental Figure 4). By Western blotting, the secretory component was not found covalently coupled to the polymeric IgA in serum, yet it was readily seen in fecal IgA. Taken together, serum IgA from BAFF-Tg mice shares some of the biochemical

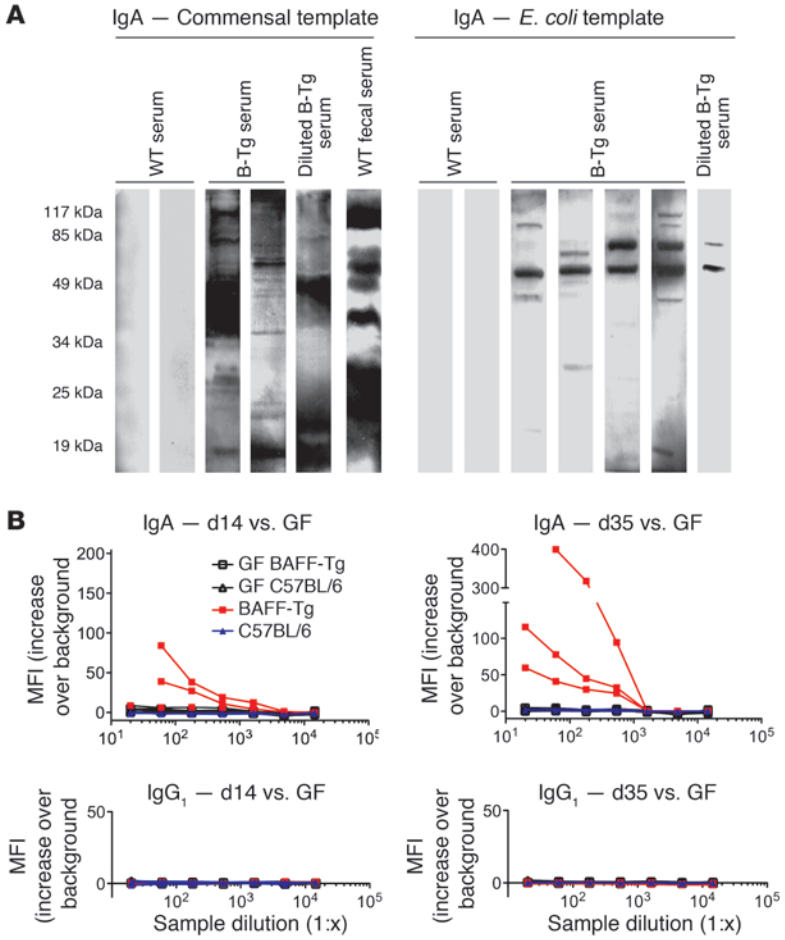

Figure 4
Evidence for commensal specificity of serum IgA from BAFF-Tg mice. (**A**) Lysed commensal bacteria or laboratory strain *E. coli* were used as the target antigens in a Western blot, using serum or fecal supernatant from WT or BAFF-2 Tg (B-Tg) mice as primary antibody and anti–IgA-HRP as secondary antibody. Blots shown are representative of 3 independent experiments. (**B**) Serum IgA (top) and IgG levels (bottom) from ASF-reconstituted GF WT mice versus BAFF-2 Tg mice were examined by flow cytometry for specific surface binding to intact *Lactobacillus murinus*, a verified bacterial species retrieved from the intestinal wash of ASF-colonized mice.

properties of IgA from patients with IgAN and some rodent models of IgAN; namely, IgA is underglycosylated, polymeric, and not associated with the secretory component.

Commensal specificity of serum IgA from BAFF-Tg mice. We speculated that the underglycosylated, polymeric IgA in the serum originated from mucosal B cells. Using a previously described Western blot protocol (37), we found that BAFF-Tg serum, but not control serum, contained IgA that was specific for components of commensal bacteria cultured from our colony (Figure 4A, left). Even when the serum was diluted to normalize total IgA concentration to WT levels, commensal specificity was still observed in the BAFF-Tg serum. Similar results were observed for an *E. coli* bacterial template, indicating that serum IgA from BAFF-Tg mice recognized common cross-reactive bacterial antigens (Figure 4A, right). Interestingly, whereas kidney homogenates from WT mice exhibited no commensal-reactive IgA, kidney homogenates derived from specific-pathogen free (SPF) BAFF-Tg kidneys showed evidence of broad reactivity to both a commensal flora template as well as an *E. coli* template (Supplemental Figure 5). A FACS-based analysis of commensal specificity using a monoculture was used to confirm our Western blot results (38). Specifically, we took advantage of WT and BAFF-Tg mice that had been rederived to germ-free (GF) status and housed in a GF facility. In the absence of preexisting commensal bacteria, GF BAFF-Tg mice were then colonized with a limited commensal microbiota (altered Schaedler flora [ASF]) that included *Lactobacillus murinus* (see below). We found that serum IgA from ASF-colonized BAFF-Tg mice bound specifically to *L. murinus* isolated from these mice, particularly at later time points after commensal reintroduction, whereas we did not detect any *L. murinus* binding with WT serum IgA (Figure 4B, top). Moreover, *L. murinus*–specific IgA was not observed in GF animals (Figure 4B, top), and commensal specificity of IgA was not observed when serum or kidney IgA were derived from GF mice (Supplemental Figure 5). Because there was no binding of BAFF-Tg serum IgG to *L. murinus* (Figure 4B, bottom), it is doubtful that the presence of commensal-specific IgA in the serum from BAFF-Tg mice was a result of a breakdown in commensal containment within the lumen of the gut. This hypothesis is consistent with the absence of secretory component in serum IgA preparations (Supplemental Figure 4).

Commensal signals are required for serum hyper-IgA and renal IgA deposition in BAFF-Tg mice. In support of the presence of commensal-specific serum IgA, BAFF-Tg mice have an increased percentage of B cells in mucosal lymphoid tissues, including the LP and the MLNs as well as the previously characterized expansion in the spleen (Supplemental Figure 6A). Combined with the observations that IgA$^+$ PCs in BAFF-Tg mice are increased histologically in the LP mice (26), in MLN by FACS and by qPCR of the secreted splice form of the IgA chain (Supplemental Figure 6, B and C), these results suggested that elevated serum IgA in these mice may be explained by increased anticommensal IgA responses in the gut. To confirm this, we examined serum IgA levels in GF BAFF-Tg mice and found that serum IgA was decreased approximately 100 fold compared with that of SPF BAFF-Tg mice, and serum IgA levels from GF BAFF-Tg mice were similar to those for GF WT mice (Figure 5A). Furthermore, the increased frequency of IgA$^+$ PCs in the gut and the deposition of IgA in the glomeruli were ablated in the GF BAFF-Tg mice (Figure 5, B–D). Interestingly, BAFF-driven B cell hyperplasia in the spleen was not affected by commensal signals. For example, like SPF BAFF-Tg mice, GF BAFF-Tg mice had significant increases in the total splenic B cell compartment as well as in the expanded percentages of splenic marginal zone B (MZB) cells and transitional 2 B cells (T2 B cells) (Supplemental Figure 7). In support of this finding, low levels of BAFF, e.g., in female BAFF-1 mice, that were inadequate to drive increases in serum IgA levels and renal injury were sufficient to expand the MZB and T2 B cell populations and the B cell compartment (data not shown). Therefore, the basic compartmental expansion and shifts in splenic MZB and T2 B cell percentages are not coupled to

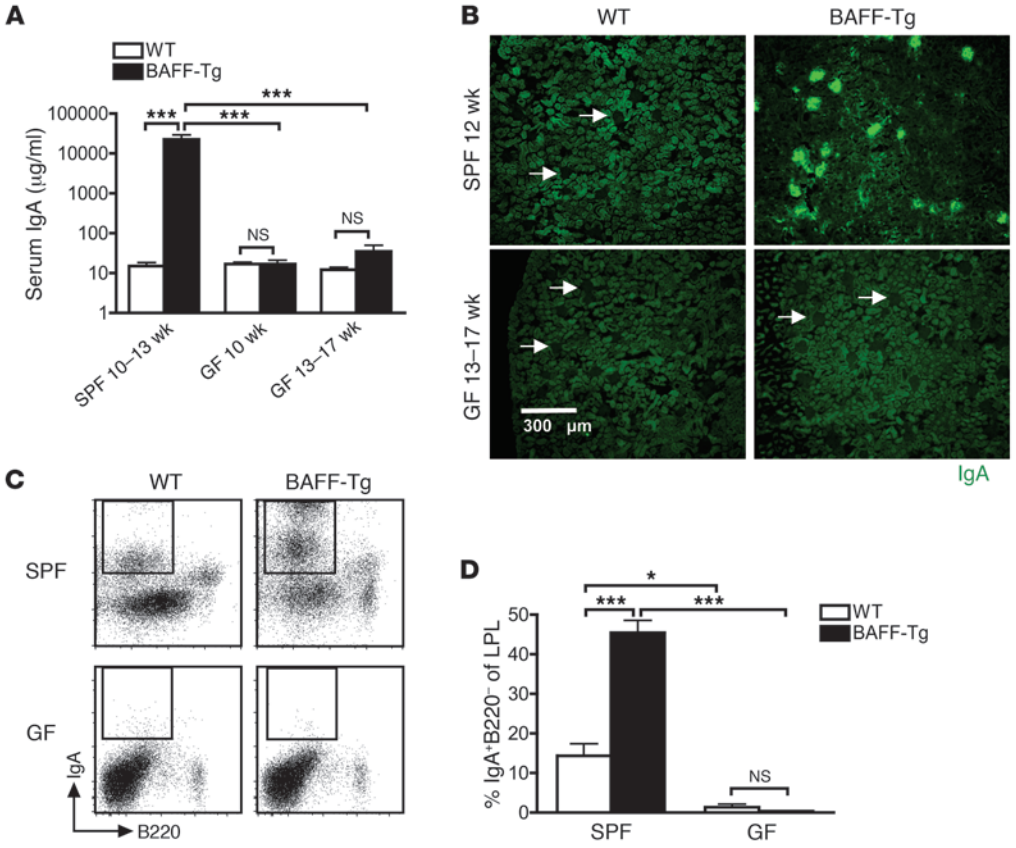

Figure 5

Commensal bacteria are necessary for hyper-IgA syndrome in BAFF-Tg mice. (**A**) Serum IgA measured from SPF and GF C57BL/6 (WT) and BAFF-2 Tg mice measured by ELISA. At least 4 mice were analyzed per group (***$P < 0.001$). (**B**) Immunofluorescence staining of frozen sections of kidneys from SPF and GF C57BL/6 and BAFF-2 Tg mice stained for IgA (green). Images are representative of analysis of at least 8 mice per group (original magnification, ×100). Arrows identify glomeruli that do not exhibit IgA deposition. (**C**) Representative FACS profiles of IgA$^+$ PCs in the gut LP of SPF versus GF C57BL/6 and BAFF-2 Tg mice. (**D**) Quantification of IgA$^+$ PCs from **C**. Analysis was performed on 12-week-old BAFF-2 Tg mice versus C57BL/6 mice. Note that BAFF levels in GF BAFF-2 Tg mice were approximately equal to those observed for SPF BAFF-Tg mice (1,733.2 ± 660.8 pg/ml; n =12). LPL, LP lymphocyte. Bars in **A** and **D** represent the mean ± SEM. *$P < 0.05$, ***$P < 0.001$.

the high IgA phenotype in BAFF-Tg mice. Furthermore, IgA deposition in the kidney is not driven by BAFF alone and depends on the presence of bacterial signals or antigens.

To determine whether commensal flora could reestablish the hyper-IgA phenotype in adult BAFF-Tg mice, GF mice were colonized with ASF at 6 weeks of age, and serum IgA levels were tracked over the subsequent 6.5 weeks. Prior to colonization, GF WT and BAFF-Tg mice both had low serum IgA levels (Figure 6A). However, after only 2 weeks, colonized BAFF-Tg mice exhibited substantially increased levels of serum IgA that continued to increase until about 3.5 weeks, at which point, they stabilized. Conversely, serum IgA levels did not dramatically increase in WT mice over this period. The increase in serum IgA in BAFF-Tg mice was accompanied by a significant increase in the frequency of IgA$^+$ PCs in the LP (Figure 6, B and C) and a reemergence of renal glomerular IgA deposition (Figure 6D). We also examined the emergence of IgA$^+$ PCs in different anatomical compartments at an early time point after colonization. Interestingly, as little as 8 days after colonization, IgA$^+$ PCs were detected in mucosal tissues of BAFF-Tg mice at levels that approach those of SPF BAFF-Tg mice, suggesting that the expansion of IgA$^+$ PCs occurs very rapidly in response to commensal flora. The intestinal LP represented the richest source of IgA$^+$ PCs, followed by the PP and MLNs (Figure 6, E and F). While conventionally housed SPF BAFF-Tg mice displayed widespread dissemination of IgA$^+$ PCs in the periphery, the peripheral tissues of GF BAFF-Tg mice did not show evidence of IgA$^+$ PCs at 8 days after colonization (Figure 6F). Therefore, the BAFF-driven hyper-IgA syndrome in these mice is not developmentally determined but is strongly influenced by ongoing commensal-dependent signals in the intestine.

IgA is a critical component of the kidney pathology in BAFF-Tg mice. To provide direct evidence that elevated synthesis of IgA and renal pathology are coupled, we crossed BAFF-Tg mice with IgA-deficient mice. BAFF-Tg, *IgA*$^{-/-}$, and BAFF-Tg × *IgA*$^{-/-}$ male mice were aged to 14–15 months, with a subgroup analyzed at 8–10 months. We found that hematuria and urinary protein and albumin levels were appreciably reduced in BAFF-Tg mice that lacked IgA (Figure 7). Decreased urine urea nitrogen and urine creatinine levels in BAFF-Tg mice were also normalized on the IgA-deficient background, although the spot urine collection did not allow for compensation of the hydration status for these 2 measurements (data not shown). Curiously, proteinuria in *IgA*$^{-/-}$ mice was substantially

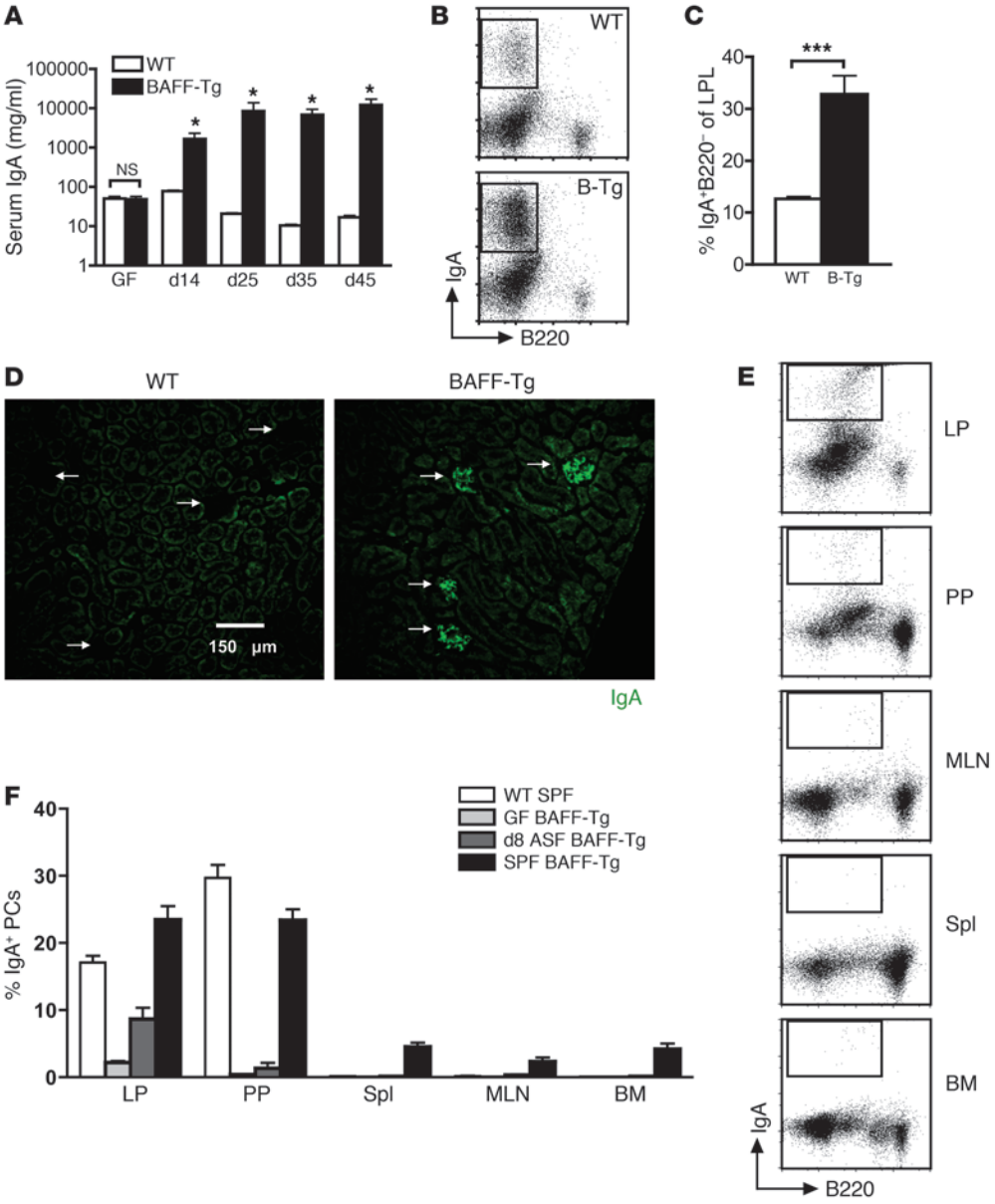

Figure 6
Hyper-IgA phenotype in BAFF-Tg mice is restored upon recolonization with commensal flora. (**A**) Average serum IgA levels in GF C57BL/6 (n = 5) and BAFF-2 Tg (n = 7) mice after introduction of ASF at 6 weeks of age as measured by ELISA. *P < 0.05. (**B**) Representative FACS and (**C**) frequency of IgA+ PCs isolated from small intestinal LP of C57BL/6 and BAFF-2 Tg mice after 45 days of recolonization. ***P < 0.01. (**D**) Representative images of IgA immunofluorescence staining of frozen sections of kidneys from C57BL/6 and BAFF-2 Tg mice recolonized for 45 days (original magnification, ×200). Arrows indicate individual glomeruli. (**E**) Representative FACS analysis and (**F**) quantification of IgA+ PCs in different anatomical sites after commensal recolonization contrasted with SPF BAFF-2 Tg mice. A GF reconstitution experiment was performed twice with similar results on 8-week-old BAFF-2 Tg mice versus age-matched C57BL/6 mice. Spl, spleen. Bars in **A**, **C**, and **F** represent the mean ± SEM.

lower than that in matched $IgA^{+/+}$ mice, regardless of whether the data were or were not corrected for hydration status using the creatinine ratio. At 8 to 10 months, the sera from these BAFF-1 × $IgA^{+/+}$ mice exhibited serum hyper-IgA, and IgA deposits were readily seen in the kidney (Supplemental Figure 8B). Serum BAFF levels remained also high (data not shown). Histological examination of the glomeruli was consistent with reduced disease in the aged BAFF-Tg $IgA^{-/-}$ cohorts, although a small subset of BAFF-Tg $IgA^{-/-}$ mice had elevated urinary protein and, like the BAFF-Tg $IgA^{+/+}$ mice, still retained interstitial tubular F4/80-positive monocytic infiltrates (Supplemental Figure 8, D and E). We next examined BAFF-Tg $IgA^{+/+}$ versus BAFF-Tg $IgA^{-/-}$ mice at 14 to 15 months of age. At this time point, we observed a drop in serum IgA levels in BAFF-Tg $IgA^{+/+}$ mice (Supplemental Figure 8A), likely due to reduced BAFF expression correlating with a loss of testosterone-driven sexual dimorphism in the kidney. Nevertheless, IgG, IgA, and IgM immune complex (IC) deposits in the glomeruli at 14 to 15 months were similar to those in mice at 8 to 10 months, except that IgG deposition was commonly observed in the $IgA^{-/-}$ setting (Supplemental Figure 8B). Taken together, BAFF-Tg mice exhibited impaired kidney function (measured at 14 to 15 months) that was preceded by an elevation in serum IgA at 8 to 10 months; however, on an $IgA^{-/-}$ background, BAFF overexpression was not sufficient to mediate the full manifestation of kidney dysfunction. These data indicate that IgA is a key component of the development of renal disease in these mice.

APRIL and to a lesser extent BAFF are elevated in the serum from patients with IgAN. BAFF levels have been shown to be elevated in sera of patients with autoimmune disorders such as Sjögren's syndrome, rheumatoid arthritis, and SLE (39). Furthermore, two studies hint at a correlation between BAFF and IgAN. Specifically, serum BAFF levels were found to be weakly correlated with serum IgA levels in patients with IgAN undergoing tonsillectomy (40), and monocytes from patients with IgAN were found to produce more BAFF in

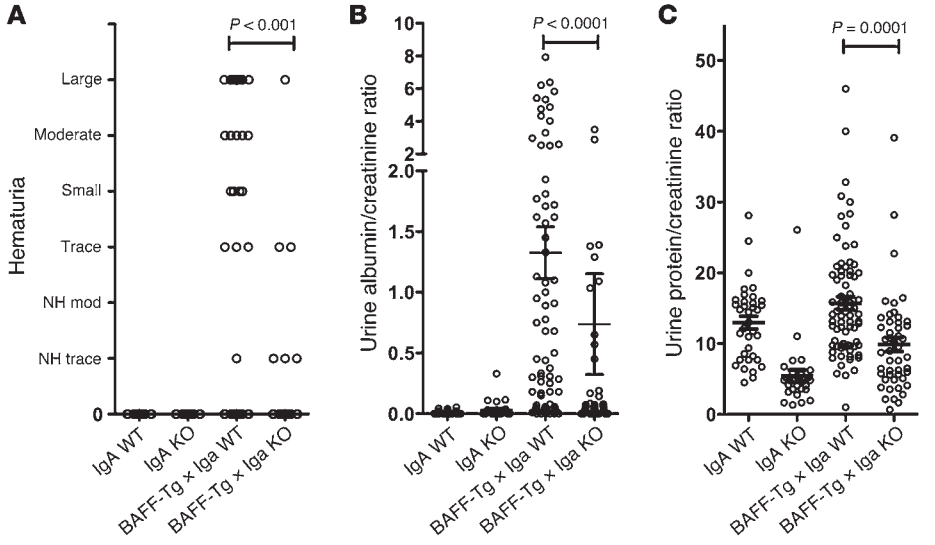

Figure 7
Loss of IgA restores kidney function in BAFF-Tg mice. Male BAFF-1 Tg mice bred onto a WT or IgA-deficient background were assessed at 13.5 to 15 months of age for the renal damage parameters: (**A**) hematuria, (**B**) urinary ratio of microalbumin/creatinine, and (**C**) urinary ratio of total protein/creatinine. 36 *IgA*$^{+/+}$, 28 *IgA*$^{-/-}$, 72 BAFF-Tg × *IgA*$^{+/+}$, and 48 BAFF-Tg × *IgA*$^{-/-}$ mice were used, except for hematuria assessment, for which 21 *IgA*$^{+/+}$, 23 *IgA*$^{-/-}$, 50 BAFF-Tg × *IgA*$^{+/+}$, and 33 BAFF-Tg × *IgA*$^{-/-}$ animals were analyzed ± SEM. Individual symbols represent individual mice; horizontal bars represent the mean ± SEM.

response to CpG-ODN (41). An ELISA analysis of sera from 2 separate cohorts of patients with IgAN showed a modest increase in BAFF protein in cohort 1 compared with that in control samples (Figure 8). We noted a slight gender bias in the controls of cohort 1, with females having 1.7 fold the amount of BAFF in male sera ($P < 0.001$). Controls from cohort 2 were almost entirely female. Because BAFF and APRIL can both bind to TACI and BCMA and TACI is critical for IgA switch in mice, we examined the related molecule APRIL. In both cohorts, a subset of patients with IgAN (14%–18%) had serum APRIL levels 3- to 20-fold above those of the non-IgAN controls when measured by ELISA. Within the patients with IgAN in cohort 2, gender, hypertensive status, and macroscopic hematuria were not correlated with either cytokine. However, APRIL levels in patients with IgAN (cohort 2) were significantly correlated with age ($r = 0.271$, $P = 0.008$), serum creatinine ($r = 0.517$, $P < 0.001$), and urine protein/creatinine ratio ($P = 0.008$) and marginally significant for urine protein ($r = 0.206$, $P = 0.053$). Thus, at some stage in IgAN, or in a subset of patients with IgAN, APRIL levels become elevated and may contribute to the pathology.

Discussion

Given the recent success in the treatment of lupus patients with BAFF inhibitors, there is considerable interest in the lupus-like disease arising in BAFF-Tg mice. Taking advantage of the variability between 2 founder lines and gender differences in BAFF-Tg mice, we found that the tipping point for the manifestation of renal pathology and premature death was the level of BAFF protein in the serum. Slight increases in BAFF expression were sufficient to expand the B cell compartment size, yet high BAFF levels correlated with vastly increased serum IgA levels, glomerular IgA$^+$ IC deposition, and kidney pathology. Furthermore, kidney function was improved when BAFF-Tg mice were crossed onto an IgA-deficient background. Interestingly, MRL/lpr mice with renal disease had 100–400 ng/ml BAFF in the blood (Supplemental Figure 1C), and, indeed, serum IgA levels were also elevated to about 1 mg/ml (data not shown). MRL/lpr mice are reported to have increased numbers of IgA-secreting cells, excess IgA rheumatoid factor (Rf), and IgA deposition in the kidney glomeruli, suggesting that a facet of the pathology manifested in the BAFF-Tg mice also appears in the MRL/lpr lupus strain (42, 43).

We also observed that serum IgA in BAFF-Tg mice is polymeric and underglycosylated, and both properties are features of human IgAN. Therefore, we propose that BAFF-Tg mice may model some aspects of human IgAN and provide some clues that may help investigators understand this common renal disease. Consistent with this reasoning, APRIL, and to a lesser extent BAFF, concentrations were elevated in the serum of patients with IgAN. These conclusions require some reconciliation with the long history of BAFF-Tg mice as a model of SLE, the effects of BAFF-R signaling on the BCR set point for self-reactivity, elevated BAFF levels in the blood of SLE patients, and, indeed, the recent clinical success of a BAFF-blocking antibody. The 2 separate colonies used in this study effectively lack IgG autoantibodies and fail to display signs of salivary gland infiltration — both properties of the original colony. However, these mice do retain the same expanded B cell compartment size and enlarged PP. Both genetic background and environmental factors may have played a role in this shift. Analysis of the colony survival at 2 times without further backcrossing showed a drift to less severe disease, pointing toward environmental changes (see discussion in the Supplemental Methods). Interestingly, the current BAFF-1 and BAFF-2 homozygous transgene colonies stemmed from mice that had been rederived to remove potential infection with *Helicobacter* and *Pasturella*, organisms that were endemic in many colonies at that time. Because both founders, each with differing sites for integration of the transgene, now display a milder phenotype, we reason that drift in environmental/commensal factors, rather than genetic background, underlies the colony differences. We hypothesize that the role of IgA deposition in kidney pathology in the original BAFF-Tg colony may have been mixed with or obscured by more conventional IgG-driven autoimmunity. Such interplay was recently described in the autoimmune-prone *Lyn*$^{-/-}$ mice, in which IgA glomerular deposition was observed only in the absence of IgG antinuclear antibodies (44).

We propose that there are several phenotypic levels in BAFF-Tg mice. First, low-level excess BAFF simply expands the B cell compartment, including the T2 and MZB cells, concomitant with an increase in serum IgM levels, i.e., BAFF-R–mediated events. As these mice do not have substantial renal pathology, these components are not direct drivers of disease. Second, excessive levels of BAFF

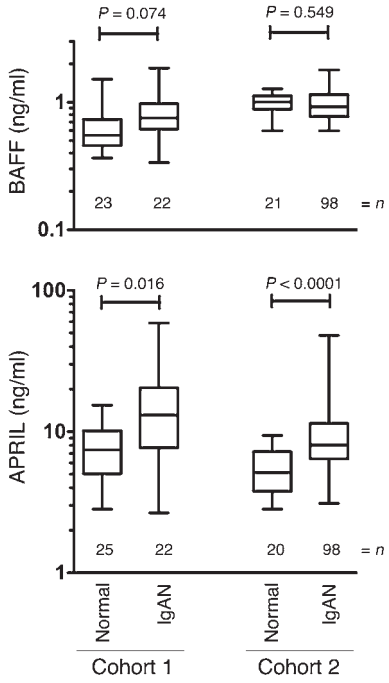

Figure 8
Elevated APRIL and less affected BAFF levels in the serum of patients with IgAN. Sera from 2 separate groups of biopsy-confirmed patients with IgAN, cohort 1 (Toronto) and cohort 2 (Alabama), were subjected to ELISA quantification of BAFF and APRIL. Box and whisker plots show the 5%–95% limits of the range, and significance was determined by the Mann-Whitney test. The numbers represent the number of patients.

lead to an IgAN-like pathology in the presence of commensal flora. Third, aspects of the colony environment or different commensal flora create conditions wherein more conventional autoimmune responses emerge and overlay or even supplant the IgAN-like phenotype with a more classical IgG autoantibody-driven kidney pathology. Thus, evaluating BAFF-Tg mice that lack the overt SLE/Sjögren's syndrome pathology provides an excellent opportunity to query the etiological drivers that lead to an IgAN phenotype.

To this end, the use of GF mice and colonization experiments proved that commensal flora were required for the initial generation of the IgA$^+$ PCs. It was posited that the gut flora are critical for APRIL expression and hence the commensal dependence for IgA switch (28). However, in our study, excess BAFF/APRIL signaling was maintained by the transgene, yet the IgA production remained commensal dependent. Therefore, BAFF is insufficient on its own to induce IgA-associated renal injury, and other commensal-sensitive components of the mucosal niche are required for IgA switch and the IgA-driven pathology to manifest. These factors could include regulation of TACI expression by local TLR/NLR signaling (22), cooperation between BAFF/APRIL and other locally produced cytokines such as TGF-β, or perhaps the collaboration of other gut-resident cells, such as intraepithelial lymphocytes, that are known to be sensitive to the commensal load of the gut lumen (45).

After colonization of BAFF-Tg mice with commensal flora, the number of IgA$^+$B220$^-$ B cells was highest in the BAFF-Tg LP compartment (which includes both the disorganized LP and the LP-resident ILF), followed by the PP and the MLN as early as 8 days after colonization. When compared with SPF mice, limited IgA$^+$B220$^-$ B cells were observed in the periphery at this stage, implying that with time, the continual generation of IgA$^+$ PCs in the BAFF-Tg gut eventually "spills over" into the periphery. Normally, commensal-specific IgA-secreting PCs do not readily seed the nonmucosal niches. The mucosal firewall is a term used to characterize the inability of both commensal antigens and commensal-reactive immune cells to traffic past the gut-draining lymph nodes (46). Our data demonstrate that the collaboration between commensal bacteria and elevated BAFF levels results in a perturbed homeostasis, with vigorous class switching to IgA in the gut. This process culminates in an aberrant widespread dissemination of IgA$^+$ PCs into the spleen, kidney, and bone marrow, i.e., a breach of the mucosal firewall. What is not clear from this work is whether gut-derived IgA switched memory B cells, plasmablasts, or terminal PCs have themselves breached the firewall and mediated this seeding.

A previous report analyzed BAFF-Tg mice crossed onto a TCRαβ × TCRγδ double-knockout background and showed that T cells were not necessary for IgG-driven kidney disease (47). These T cell–deficient BAFF-Tg mice lacked high circulating levels of IgA, and therefore it was concluded that IgA deficiency does not contribute to renal disease. We think this experiment differs substantially from our study because the T cell–deficient BAFF-Tg mice displayed IgG antinuclear antibodies, yet this aspect of the disease does not dominate our colony. It is possible that these seemingly disparate observations may reflect on an important yet ill-defined interplay between IgG and IgA immune responses, as discussed above, potentially as exemplified by the *Lyn*$^{-/-}$ mice (48).

Why should BAFF levels be tied to the numbers of IgA$^+$ PCs in these mice? Like several other TNF family members, higher-order BAFF complexes are required to trigger efficient TACI signaling (49). This enhanced receptor assembly can be provided by the large 60-mer forms of BAFF, large APRIL oligomers (if they exist), or APRIL-decorated proteoglycans (50, 51). High-molecular-weight forms of BAFF exist in BAFF-Tg mice (49), and we surmise that higher levels of transgenic BAFF expression raised the concentration of 60-mer BAFF forms and thereby enhanced TACI signaling and mucosal switching to IgA. Therefore, elevations in either APRIL or BAFF or especially highly oligomeric forms of these molecules could be pathological in the context of IgAN. Indeed, the levels of APRIL we detected in patient serum could very well be underestimated given the possibility that aggregated proteoglycan/APRIL complexes may not have been detected in our conventional ELISA system. Very little is known about the levels of large BAFF, APRIL, or potentially heteromeric BAFF/APRIL forms in human disease.

Considerable data suggest that aberrant O-linked glycosylation of the hinge region of human IgA1 makes IgA potentially nephritogenic in humans. This aberrancy may be recognized by IgG or IgA hinge region glycan- or glycopeptide-specific antibodies to form immune complexes that induce the renal injury in IgAN (52). Even though serum IgA from BAFF-Tg mice is polymeric and underglycosylated, a detractor to using mouse models for studying IgAN is that murine IgA lacks hinge region O-linked glycosylation sites and mice lack the CD89 IgA Fc receptor. One alternative possibility lies in the highly conserved N-linked glycosylation site that sits in the IgA and IgM tailpieces (53). Complete loss of glycosylation at this site results in the production of more polymeric IgA (54), and subtle changes in this region can affect glycosylation status (53). Underglycosylation of the tailpiece, or even the J chain, may enhance assembly into more unusual poly-

meric IgA forms that may be pathogenic. The polymeric IgA in BAFF-Tg mice resisted detergent dissociation, suggesting disulfide bond-mediated assembly into higher, perhaps IgM-like, oligomers. Underglycosylation could simply be uncoupled from the pathogenicity, but this seems unlikely given that a β−1-4-galactosyltransferase-1–deficient mouse develops a similar IgA-associated renal disease with expansion of the extracellular matrix in the glomeruli (55). In another mouse model, bcl2-Tg (NZW × C57BL/6)F_1, IgA is aberrantly glycosylated and becomes polymeric and pathogenic in spite of the lack of the hinge region glycosylation (36).

We speculate that the breach of the mucosal-peripheral firewall and emergence of anticommensal reactivity into the periphery may represent an important event in human immunological disease. The perturbed BAFF-APRIL signaling in the BAFF-Tg mice described here highlights one potential route to a firewall breach. While this particular breach is artificially induced, the recent discovery that TACI can directly activate MyD88 suggests that the BAFF-APRIL system may be interwoven with innate immunity and hence has the potential to be linked to commensal disequilibria. The dissemination of gut-derived IgA-secreting cells into the other peripheral organs in BAFF-Tg mice may help to reconcile varying observations in human IgAN. Some investigators have proposed a similar gut mucosa-centric etiology, while others have highlighted tonsils and bone marrow as central compartments (56). Indeed, tonsillar involvement has been proposed to explain the frequent nephritic relapses concurrent with upper respiratory tract infections in patients with IgAN (57). The airway and other mucosal compartments may also abide by similar mucosal-peripheral firewall rules, with a breach augmenting disease development. It is now more apparent that the nature of the microbiota can be a major exacerbating or ameliorating factor in the rate and extent of progression in rodent autoimmune disease (3, 58). In humans, such interplay has been suggested in intestinal, kidney (7), liver (59), and joint disease (60), and, indeed, there is mucosal firewall breach in celiac disease, which has many nonmucosal autoimmune sequelae (8, 61). These parallels between BAFF-Tg mice and human IgAN may provide a new framework to explore connections between mucosal environments and the renal pathology.

Methods

Mice. BAFF transgenic mice were originally generated as described previously, with the BAFF-1 and BAFF-2 lines being the original 816 and 823 lines, respectively (35). The transgene was driven by an ApoE enhancer coupled to the AAT promoter. Homozygous mice, as described previously (23), were obtained from Fabienne Mackay (Garvan Institute, Sidney, Australia) in 2003. BAFF-Tg mice were rederived at that point to remove potential *Helicobacter hepaticus*, *Helicobacter bilus*, and *Pasteurella pneumotropica* and maintained as the homozygous transgenics. Transgenic mice were identified by PCR as previously described (35). Homozygosity of the lines was confirmed by quantitative PCR and by FISH analysis. Both lines had a single integration site (BAFF-1, distal end of chromosome 1; BAFF-2 close to the centromere of chromosome 11). Genome scanning (The Jackson Laboratory) revealed that the 816 and 823 lines were 90% and 82% C57BL/6, respectively. The remaining DBA2 genetic contribution is retained from the original transgenic derivation using DBA2 × B6 F_1 founders.

IgA$^{-/-}$ mice were obtained from Innocent Mbawuike (Baylor University, Houston, Texas, USA) and were further backcrossed onto C57BL/6 mice for 5 generations before being rederived (Taconic). The genome of the IgA KO mice was 95% C57BL/6 by genome scan (versus the genome of 129 mice). Genotyping was performed as described previously (62). *IgA*$^{-/-}$ and homozygous BAFF-1 Tg mice were intercrossed to generate BAFF-Tg mice with an *IgA*$^{+/+}$ or *IgA*$^{-/-}$ background. The genomes of the final lines used for aging and kidney function were 92%–96% and 93%–94% C57BL/6, respectively (versus the DBA2 genome). Male mice were maintained for 13.5 to 15 months for assessment of renal function. Control WT mice were either C57BL/6 mice (The Jackson Laboratory and Charles River Laboratories) or nontransgenic littermates. (NZB/NZW)F_1 and MRL/lpr mice were purchased from The Jackson Laboratory. All mice, with the exception of GF animals (see below), were housed in sterile microisolator cages and fed sterile food and water (SPF). Mice were euthanized when albuminuria reached 2000 mg/dl or with the onset of morbidity. These criteria were used to obtain the survival data.

BAFF-2 and C57BL/6 mice were rederived into the Axenic/Gnotobiotic facility at McMaster University Health Sciences Centre and bred as GF. Briefly, GF homozygous BAFF-Tg mouse colonies were obtained by a 2-cell embryo transfer as described previously (38). Resulting litters were maintained in flexible film isolators with unlimited access to autoclaved food and water and were regularly checked for GF status by aerobic and anaerobic culture and SYTOX Green (Invitrogen) and Gram staining of cecal content to detect unculturable contamination. In addition, serological testing for known viruses and pathogens was performed periodically (Charles River Laboratories). Colonization experiments were performed by introducing mice colonized with ASF into the cages of GF mice at 6 weeks of age. All animal studies were approved by the Biogen Idec, University of Toronto, and McMaster University Institutional Animal Care and Use Committees.

Serological analyses. Serum Ig isotypes were determined by ELISA. Briefly, plates were coated with goat anti-mouse IgA, IgG, or IgM antibodies (Southern Biotech) and detected using HRP-labeled goat anti-mouse isotype-specific reagents (Southern Biotech). Standard curves were obtained using purified Ig (Southern Biotech). For evaluation of fecal IgA, fresh fecal pellets were collected and solubilized as previously described (63). IgA concentrations were assessed by ELISA as described previously for serum samples. Detection of antichromatin antibodies was performed using the QUANTA Lite Chromatin ELISA assay (NOVA Diagnostics Inc). Mouse serum samples were diluted 1:100, and captured antibodies were detected using HRP-labeled isotype-specific antibodies (SouthernBiotech). For the analysis of anti-dsDNA autoantibodies, plates were coated with methylated BSA, followed by herring sperm DNA (sheared by sonication and digested with S1 nuclease).

The extent of galactosylation of IgA was determined by a lectin-binding assay combined with ELISA. Biotinylated RCA-1 (Vector Laboratories) was used to detect terminal galactose residues as previously described (36). ELISA plates were coated with antibody to IgA, and a starting dilution of serum (adjusted to 1 μg/ml IgA) was added. When indicated, plate-bound IgA was treated with neuraminidase (*Arthrobacter ureafaciens*) at 10 mU/ml. Captured IgA was probed with biotinylated RCA-1 lectin at 10 μg/ml or biotinylated anti-mouse IgA at 1:2,500 dilution and then HRP-conjugated streptavidin. Glycosylation was expressed as a binding ratio (OD developed with lectin detection/OD developed with anti-IgA). Purified murine myeloma IgA clone S107 (Southern Biotech) was used as a poorly galactosylated control.

Size fractionation of sera was performed by chromatography on a Superose 6 column (10 mm × 300 mm; 5- to 5,000-kDa fractionation range) in PBS at a flow rate of 0.6 ml/min. 0.5-ml fractions were collected. Elution was monitored by UV absorbance and by ELISA for murine IgG, IgA, and IgM levels. Fractionation of molecular weight standards was used as a reference. Murine BAFF was quantitated by ELISA using plates coated with 2 μg/ml BCMA-human IgG1 (Biogen Idec) and blocked with PBS/5% BSA fraction V. Serially diluted serum samples were added, captured BAFF was detected with 1 μg/ml biotinylated anti-murine BAFF (Axxora), and murine recombinant BAFF (Axxora) was used as the standard (Supplemen-

tal Figure 1A). Serum mouse BAFF in Supplemental Figure 1, B and C, was quantitated using a R&D Systems ELISA Kit.

Human BAFF and APRIL serum levels were quantitated using R&D Systems and Bender MedSystems ELISA Kits, respectively. Statistical significance was assessed using the Mann-Whitney 2-tailed test.

Evaluation of commensal-specific Ig by Western blot. Western blots to determine anticommensal reactivity were performed essentially as described previously (37). In brief, commensal bacteria were cultured from fecal pellets derived from mice from our SPF colony. Bacteria were grown overnight in LB broth with shaking at 37°C and then transferred and grown to mid-log phase. Bacteria were then collected and lysed. Bacterial lysate samples were resolved by SDS-PAGE and protein transferred to a PVDF membrane by electrotransfer. Individual lanes were then cut into strips; incubated with diluted samples of serum, fecal suspension, or homogenized kidney; and then washed and incubated with HRP-conjugated anti-IgA. Finally, binding was detected using the ECL Plus Western Blot Detection System (GE Healthcare), followed by exposure to light-sensitive film and development. Developed films were scanned and images were adjusted for contrast and brightness using PhotoShop software. To compare anticommensal reactivity in the kidneys of WT and BAFF-Tg mice housed in SPF or GF facilities, representative kidneys from each group were homogenized into 1 ml of blocking buffer (PBS with 0.1% TWEEN-20 and 5% milk powder). The resulting solution was applied neat to nitrocellulose membrane strips loaded with commensal or *E. coli* template described above. IgA content of the solutions was analyzed via ELISA, as described above for serum.

Evaluation of commensal-specific Ig by flow cytometry. Commensal-specific Ig was evaluated by flow cytometry as described previously (38). Briefly, cecal contents from GF mice recolonized with ASF were assessed for presence of *Lactobacillus murinus* ASF 361 by growing overnight at 37°C under anaerobic conditions in brain-heart infusion media, and the bacterial species was subsequently confirmed by 16S rDNA analysis. 2.5×10^5 *L. murinus* bacteria per well were incubated with serial dilutions of serum samples, starting at 1:20, for 1 hour at 4°C. Plates were then washed in PBS with 2% BSA and azide (PBS/BSA) to remove any unbound Ig. The pellet was then resuspended in either 1:50 dilution of FITC–anti-IgA or 1:100 dilution of FITC–anti-IgG1 and incubated at 4°C overnight with FITC–anti-IgG1 clone A85-1 or FITC–anti-IgA clone C10-3) (all from BD Biosciences). On day 2 excess/unbound secondary antibody was washed off, and the pellet was resuspended in 100 μl PBS/BSA to be read on a FACSArray (BD Biosciences). The population was first gated using SSC-A and FSC-A, then autofluorescence was gated out in the red and FSC-W channel prior to analyzing the FITC signal. GF mice did not exhibit any *L. murinus* binding, whereas fecal IgA displayed strong reactivity to *L. murinus* (data not shown).

IgAN study participants. In the Toronto IgAN cohort (cohort 1), study patients were recruited from Toronto, Ontario, Canada; St. Etienne, France; and Helsinki, Finland, and all had biopsy-proven IgAN according to standard pathologic criteria (64). The Canadian and Finnish control subjects were derived from a large family-based genetic study of autosomal dominant polycystic kidney disease (ADPKD), and the group comprised spouses and unrelated family members without ADPKD, all with a normal urinalysis. The French control subjects were unrelated blood donors and healthy volunteers (medical staff and nurses). In the University of Alabama cohort (cohort 2), biopsy-proven patients with IgAN and healthy controls were included. In both cohorts, patients with cirrhosis, SLE, gluten enteropathy, HIV infection, and Henoch-Schönlein purpura were excluded. All study subjects gave informed consent before their blood sampling for serum analysis. The Institutional Human Subject Review Boards from both the University of Toronto and the University of Alabama approved the research protocol used in this study.

All statistical analyses used either Student's *t* or Mann-Whitney (2-tailed) methods as indicated. Further methodological details can be found in the Supplemental Methods.

Acknowledgments

We thank Kai Fu for urinalysis data; Tom Crowell and Bob Dunstan for expert analysis of the histology; Juanita Campos-Rivera, Jose Sancho (Biogen-Idec), and Dionne White (University of Toronto) for flow cytometry analysis; Veronique Bailley for HPLC sizing analyses; Irene Sizing for expert technical assistance; and Karrie Brennerman and Humphrey Gardner for pathology evaluation. This work was supported by a Kidney Foundation of Canada grant as well as a Canadian Institutes of Health Research/Instituts de Recherche en santé du Canada grant (CIHR/IRSC, MOP no. 67157) to J.L. Gommerman and a CIHR/IRSC Master's studentship to E.A. Porfilio. J. Novak, L. Novak, and B.A. Julian acknowledge grants from NIDDK, supporting their research of IgAN (DK083663, DK078244, DK080301, DK075868, DK071802, DK082753, and DK077279).

Received for publication October 27, 2010, and accepted in revised form July 13, 2011.

Address correspondence to: Jennifer Gommerman, Department of Immunology, University of Toronto, 1 King's College Circle, Toronto, Ontario, Canada. Phone: 416.978.6959; Fax: 416.978.1938; E-mail: jen.gommerman@utoronto.ca. Or to: Jeffrey Browning, Biogen Idec, 12 Cambridge Center, Cambridge, Massachusetts 02142, USA. Phone: 617.679.3312; Fax: 617.679.3148; E-mail: jeff.browning@biogenidec.com.

Melissa A.E. Lawson, Andrew J. Macpherson, and Kathy D. McCoy's present address is: Maurice Müller Laboratories (DKF), Universitätsklinik für Viszerale Chirurgie und Medizin Inselspital, University of Bern, Bern, Switzerland.

1. Fagarasan S, Kawamoto S, Kanagawa O, Suzuki K. Adaptive immune regulation in the gut: T cell-dependent and T cell-independent IgA synthesis. *Annu Rev Immunol*. 2010;28:243–273.
2. Macpherson AJ, McCoy KD, Johansen FE, Brandtzaeg P. The immune geography of IgA induction and function. *Mucosal Immunol*. 2008;1(1):11–22.
3. Chervonsky AV. Influence of microbial environment on autoimmunity. *Nat Immunol*. 2010;11(1):28–35.
4. Brandtzaeg P. Function of mucosa-associated lymphoid tissue in antibody formation. *Immunol Invest*. 2010;39(4–5):303–355.
5. Yuvaraj S, et al. Evidence for local expansion of IgA plasma cell precursors in human ileum. *J Immunol*. 2009;183(8):4871–4878.
6. Sanders JT, Wyatt RJ. IgA nephropathy and Henoch-Schoenlein purpura nephritis. *Curr Opin Pediatr*. 2008;20(2):163–170.
7. Wang J, et al. Dysregulated LIGHT expression on T cells mediates intestinal inflammation and contributes to IgA nephropathy. *J Clin Invest*. 2004; 113(6):826–835.
8. Brandtzaeg P. Update on mucosal immunoglobulin A in gastrointestinal disease. *Curr Opin Gastroenterol*. 2010;26(6):554–563.
9. Patricio P, Ferreira C, Gomes MM, Filipe P. Autoimmune bullous dermatoses: a review. *Ann N Y Acad Sci*. 2009;1173:203–210.
10. Le Loet X, et al. Serum IgA rheumatoid factor and pyridinoline in very early arthritis as predictors of erosion(s) at two years: a simple model of prediction from a conservatively treated community-based inception cohort. *Arthritis Care Res (Hoboken)*. 2010; 62(12):1739–1747.
11. Sharman A, Furness P, Feehally J. Distinguishing C1q nephropathy from lupus nephritis. *Nephrol Dial Transplant*. 2004;19(6):1420–1426.
12. Tomana M, Novak J, Julian BA, Matousovic K, Konecny K, Mestecky J. Circulating immune complexes in IgA nephropathy consist of IgA1 with galactose-deficient hinge region and antiglycan antibodies. *J Clin Invest*. 1999;104(1):73–81.
13. Smith AC, de Wolff JF, Molyneux K, Feehally J, Barratt J. O-glycosylation of serum IgD in IgA nephropathy. *J Am Soc Nephrol*. 2006;17(4):1192–1199.
14. Oortwijn BD, et al. Differential glycosylation of polymeric and monomeric IgA: a possible role in glomerular inflammation in IgA nephropathy.

J Am Soc Nephrol. 2006;17(12):3529–3539.
15. Narita I, Gejyo F. Pathogenetic significance of aberrant glycosylation of IgA1 in IgA nephropathy. *Clin Exp Nephrol*. 2008;12(5):332–338.
16. Novak J, Julian BA, Tomana M, Mestecky J. IgA glycosylation and IgA immune complexes in the pathogenesis of IgA nephropathy. *Semin Nephrol*. 2008;28(1):78–87.
17. Feehally J, Allen AC. Structural features of IgA molecules which contribute to IgA nephropathy. *J Nephrol*. 1999;12(2):59–65.
18. Iwasato T, Arakawa H, Shimizu A, Honjo T, Yamagishi H. Biased distribution of recombination sites within S regions upon immunoglobulin class switch recombination induced by transforming growth factor beta and lipopolysaccharide. *J Exp Med*. 1992; 175(6):1539–1546.
19. Castigli E, et al. Impaired IgA class switching in APRIL-deficient mice. *Proc Natl Acad Sci U S A*. 2004; 101(11):3903–3908.
20. Castigli E, et al. TACI and BAFF-R mediate isotype switching in B cells. *J Exp Med*. 2005;201(1):35–39.
21. Litinskiy MB, et al. DCs induce CD40-independent immunoglobulin class switching through BLyS and APRIL. *Nat Immunol*. 2002;3(9):822–829.
22. Mackay F, Schneider P. Cracking the BAFF code. *Nat Rev Immunol*. 2009;9(7):491–502.
23. Batten M, et al. TNF deficiency fails to protect BAFF transgenic mice against autoimmunity and reveals a predisposition to B cell lymphoma. *J Immunol*. 2004;172(2):812–822.
24. Do RK, Hatada E, Lee H, Tourigny MR, Hilbert D, Chen-Kiang S. Attenuation of apoptosis underlies B lymphocyte stimulator enhancement of humoral immune response. *J Exp Med*. 2000;192(7):953–964.
25. Fletcher CA, et al. Development of nephritis but not sialadenitis in autoimmune-prone BAFF transgenic mice lacking marginal zone B cells. *Eur J Immunol*. 2006;36(9):2504–2514.
26. McCarthy DD, Chiu S, Gao Y, Summers-deLuca LE, Gommerman JL. BAFF induces a hyper-IgA syndrome in the intestinal lamina propria concomitant with IgA deposition in the kidney independent of LIGHT. *Cell Immunol*. 2006;241(2):85–94.
27. Castigli E, et al. TACI is mutant in common variable immunodeficiency and IgA deficiency. *Nat Genet*. 2005;37(8):829–834.
28. He B, et al. Intestinal bacteria trigger T cell-independent immunoglobulin A(2) class switching by inducing epithelial-cell secretion of the cytokine APRIL. *Immunity*. 2007;26(6):812–826.
29. He B, et al. The transmembrane activator TACI triggers immunoglobulin class switching by activating B cells through the adaptor MyD88. *Nat Immunol*. 2010;11(9):836–845.
30. Xavier RJ, Podolsky DK. Unravelling the pathogenesis of inflammatory bowel disease. *Nature*. 2007; 448(7152):427–434.
31. Gabrielsen AE, Simmons AD, Rudofsky UH. C4 in glomerular lesions of NZB/NZW mice. *Clin Exp Immunol*. 1977;27(2):222–226.
32. Enzler T, et al. Alternative and classical NF-kappa B signaling retain autoreactive B cells in the splenic marginal zone and result in lupus-like disease. *Immunity*. 2006;25(3):403–415.
33. Khare SD, et al. Severe B cell hyperplasia and autoimmune disease in TALL-1 transgenic mice. *Proc Nat Acad Sci*. 1999;97(7):3370–3375.
34. Stohl W, Jacob N, Guo S, Morel L. Constitutive overexpression of BAFF in autoimmune-resistant mice drives only some aspects of systemic lupus erythematosus-like autoimmunity. *Arthritis Rheum*. 2010; 62(8):2432–2442.
35. Mackay F, et al. Mice transgenic for BAFF develop lymphocytic disorders along with autoimmune manifestations. *J Exp Med*. 1999;190(11):1697–1710.
36. Marquina R, et al. Inhibition of B cell death causes the development of an IgA nephropathy in (New Zealand white x C57BL/6)F(1)-bcl-2 transgenic mice. *J Immunol*. 2004;172(11):7177–7185.
37. Macpherson AJ, Gatto D, Sainsbury E, Harriman GR, Hengartner H, Zinkernagel RM. A primitive T cell-independent mechanism of intestinal mucosal IgA responses to commensal bacteria. *Science*. 2000; 288(5474):2222–2226.
38. Slack E, et al. Innate and adaptive immunity cooperate flexibly to maintain host-microbiota mutualism. *Science*. 2009;325(5940):617–620.
39. Moisini I, Davidson A. BAFF: a local and systemic target in autoimmune diseases. *Clin Exp Immunol*. 2009;158(2):155–163.
40. Goto T, Bandoh N, Yoshizaki T, Takahara M, Nonaka S, Harabuchi Y. Therapeutic effects and prognostic factors in tonsillectomy patients with IgA nephropathy. *Nippon Jibiinkoka Gakkai Kaiho*. 2007;110(2):53–59.
41. Goto T, et al. Increase in B-cell-activation factor (BAFF) and IFN-gamma productions by tonsillar mononuclear cells stimulated with deoxycytidyl-deoxyguanosine oligodeoxynucleotides (CpG-ODN) in patients with IgA nephropathy. *Clin Immunol*. 2008;126(3):260–269.
42. Boackle SA, et al. CR1/CR2 deficiency alters IgG3 autoantibody production and IgA glomerular deposition in the MRL/lpr model of SLE. *Autoimmunity*. 2004;37(2):111–123.
43. Jonsson R, Pitts A, Mestecky J, Koopman W. Local IgA and IgM rheumatoid factor production in autoimmune MRL/lpr mice. *Autoimmunity*. 1991; 10(1):7–14.
44. Oracki SA, et al. CTLA4Ig alters the course of autoimmune disease development in $Lyn^{-/-}$ mice. *J Immunol*. 2010;184(2):757–763.
45. Suzuki H, Jeong KI, Itoh K, Doi K. Regional variations in the distributions of small intestinal intraepithelial lymphocytes in germ-free and specific pathogen-free mice. *Exp Mol Pathol*. 2002;72(3):230–235.
46. Macpherson AJ, Slack E, Geuking MB, McCoy KD. The mucosal firewalls against commensal intestinal microbes. *Semin Immunopathol*. 2009;31(2):145–149.
47. Groom JR, et al. BAFF and MyD88 signals promote a lupuslike disease independent of T cells. *J Exp Med*. 2007;204(8):1959–1971.
48. Tsantikos E, Oracki SA, Quilici C, Anderson GP, Tarlinton DM, Hibbs ML. Autoimmune disease in Lyn-deficient mice is dependent on an inflammatory environment established by IL-6. *J Immunol*. 2010; 184(3):1348–1360.
49. Bossen C, et al. TACI, unlike BAFF-R, is solely activated by oligomeric BAFF and APRIL to support survival of activated B cells and plasmablasts. *Blood*. 2008; 111(3):1004–1012.
50. Mackay F, Schneider P. TACI, an enigmatic BAFF/APRIL receptor, with new unappreciated biochemical and biological properties. *Cytokine Growth Factor Rev*. 2008;19(3–4):263–276.
51. Sakurai D, Hase H, Kanno Y, Kojima H, Okumura K, Kobata T. TACI regulates IgA production by APRIL in collaboration with HSPG. *Blood*. 2007; 109(7):2961–2967.
52. Suzuki H, et al. Aberrantly glycosylated IgA1 in IgA nephropathy patients is recognized by IgG antibodies with restricted heterogeneity. *J Clin Invest*. 2009;119(6):1668–1677.
53. Yoo EM, et al. Structural requirements for polymeric immunoglobulin assembly and association with J chain. *J Biol Chem*. 1999;274(47):33771–33777.
54. Chuang PD, Morrison SL. Elimination of N-linked glycosylation sites from the human IgA1 constant region: effects on structure and function. *J Immunol*. 1997;158(2):724–732.
55. Nishie T, et al. Development of immunoglobulin A nephropathy- like disease in beta-1,4-galactosyltransferase-I-deficient mice. *Am J Pathol*. 2007; 170(2):447–456.
56. Suzuki Y, Tomino Y. Potential immunopathogenic role of the mucosa-bone marrow axis in IgA nephropathy: insights from animal models. *Semin Nephrol*. 2008;28(1):66–77.
57. Bene MC, Faure GC, Hurault de Ligny B, de March AK. Clinical involvement of the tonsillar immune system in IgA nephropathy. *Acta Otolaryngol Suppl*. 2004;555(555):10–14.
58. Wu HJ, et al. Gut-residing segmented filamentous bacteria drive autoimmune arthritis via T helper 17 cells. *Immunity*. 2010;32(6):815–827.
59. Adams DH, Eksteen B, Curbishley SM. Immunology of the gut and liver: a love/hate relationship. *Gut*. 2008;57(6):838–848.
60. Hvatum M, Kanerud L, Hallgren R, Brandtzaeg P. The gut-joint axis: cross reactive food antibodies in rheumatoid arthritis. *Gut*. 2006;55(9):1240–1247.
61. Green PH, Jabri B. Celiac disease. *Annu Rev Med*. 2006;57:207–221.
62. Harriman GR, et al. Targeted deletion of the IgA constant region in mice leads to IgA deficiency with alterations in expression of other Ig isotypes. *J Immunol*. 1999;162(5):2521–2529.
63. Kang HS, et al. Signaling via LTbetaR on the lamina propria stromal cells of the gut is required for IgA production. *Nat Immunol*. 2002;3(6):576–582.
64. Liu XQ, et al. IL5RA and TNFRSF6B gene variants are associated with sporadic IgA nephropathy. *J Am Soc Nephrol*. 2008;19(5):1025–1033.